Unified theory for the scaling of the crossover between strong and weak disorder behaviors of optimal paths and directed or undirected polymers in disordered media

Daniel Villarrubia-Moreno [1] and Pedro Córdoba-Torres [2,*]

[1]*Departamento de Matemáticas and Grupo Interdisciplinar de Sistemas Complejos (GISC), Universidad Carlos III de Madrid, Leganés 28911, Spain*

[2]*Departamento de Física Matemática y de Fluidos, Universidad Nacional de Educación a Distancia (UNED), Las Rozas 28232, Spain*

(Received 24 June 2024; accepted 15 August 2024; published 11 September 2024)

In this paper, we are concerned with the crossover between strong disorder (SD) and weak disorder (WD) behaviors in three well-known problems that involve minimal paths: directed polymers (directed paths with fixed starting point and length), optimal paths (undirected paths with a fixed end-to-end or spanning distance), and undirected polymers (undirected paths with a fixed starting point and length). We present a unified theoretical framework from which we can easily deduce the scaling of the crossover point of each problem in an arbitrary dimension. Our theory is based on the fact that the SD limit behavior of these systems is closely related to the corresponding percolation problem. As a result, the properties of those minimal paths are completely controlled by the so-called red bonds of percolation theory. Our model is first addressed numerically and then approximated by a two-term approach. This approach provides us with an analytical expression that seems to be reasonably accurate. The results are in perfect agreement with our simulations and with most of the results reported in related works. Our research also leads us to propose this crossover point as a universal measure of the disorder strength in each case. Interestingly, that measure depends on both the statistical properties of the disorder and the topological properties of the network.

DOI: 10.1103/PhysRevE.110.034502

I. INTRODUCTION

Minimal paths in disordered systems have been investigated for decades due to their broad spectrum of applications which include the following: polymer science [1], transport [2–4], fluid flow through porous media [5,6], human behavior [7], social networks [8], communication networks [9–12], and traffic engineering [4,12–14].

Disordered systems are modeled by regular lattices or random networks whose bonds are assigned a positive random weight w. Bond weights are usually considered as independent and identically distributed (i.i.d.) random variables with common probability density $f(w)$, cumulative distribution $F(w)$ with $F(0) = 0$, and support $[w_A, w_B]$ with $w_A \geqslant 0$.

The notion of a minimal path here refers to the path that minimizes the sum of the weights along it. The minimal sum is the total weight of the minimal path and is denoted by W_{opt}. The optimization is carried out over the ensemble of paths that are compatible with the geometrical constraints of the problem. These constraints thus determine the kind of problem. In this paper, we are interested in the following three problems:

(i) *Directed polymers in random media* (DPRM), a paradigm of the directed problem [15]. The starting point and the length of the path are fixed, but the ending point is not fixed. In $(\mathcal{D}+1)$-dimensional DPRM, the lattice bonds are directed in a selected direction (the longitudinal direction) which is usually referred to as time t. By construction, t accounts for the length of the polymer. The transverse hyperplane with dimension $\mathcal{D}$ is usually referred to as space x.

(ii) *Optimal paths* (OPs) [16,17]. We distinguish between OPs in regular lattices (OPRL*s*) and OPs in random networks (OPRN*s*). In $\mathcal{D}$-dimensional OPRL*s*, we have two principal scenarios. We may consider the optimal path connecting two opposite sides of a $\mathcal{D}$-dimensional lattice of linear size L. In that case, there is a single length scale given by the *spanning distance* L. But we may also consider the optimal path between two fixed sites separated by an *end-to-end distance* r in a $\mathcal{D}$-dimensional lattice with arbitrary size $L_1 \times L_2 \times \cdots \times L_{\mathcal{D}}$. In that case, we have two relevant length scales: r and $\min_i\{L_i\}$ [18]. The scaling of the optimal path in the first case is the same as that obtained in the second problem when we consider $r = \min_i\{L_i\} = L$ [18]. In both cases, the length of the optimal path is given by the number of bonds along it (hopcount) and its mean is denoted by ℓ_{opt}. In the OPRN problem, we consider a random network of size N (number of nodes) and ℓ_{opt} accounts for the average length of the optimal path between two nodes in the network. In all cases, optimal paths are *self-avoiding walks* (SAWs) with no length restriction.

(iii) *Undirected polymers in random media* (UPRM) [19–22]. They are the undirected analogs of DPRM. In $\mathcal{D}$-dimensional UPRM, we consider a polymer of fixed length ℓ that is attached by one end to the center of a $\mathcal{D}$-dimensional lattice. The configurations of the polymer are SAWs with a fixed starting point and length and free end point.

There has been much interest in the effect of the disorder on the geometry of these minimal paths [17–20,23–26]. It is known that their scaling properties undergo a crossover

*Contact author: pcordoba@dfmf.uned.es

between two regimes: the weak disorder (WD) regime, in which almost all links contribute to W_{opt}, and the strong disorder (SD) regime, which is obtained from extremely broad distributions, so we can assume that the total weight of the path is dominated by the maximum value of w along it, $W_{\text{opt}} = w_{\text{max}}$ (we call it the max principle). Note that the max principle is rigorously valid only in the ultrametric limit, also called the SD limit [27]. While in WD conditions there is no single bond whose removal yields a significant change in the minimal path, in the SD case such a bond always exists.

The scaling in the WD regime depends on the kind of problem. OPRL*s* in WD belong to the same *universality class* as DPRM [23,28,29], which can be mapped to the celebrated Kardar-Parisi-Zhang (KPZ) universality class [15,30]. In both cases, the minimal paths are self-affine curves. On the other hand, UPRM in WD conditions are fractal, and their fractal dimension is smaller than that of SAWs without disorder [19,22].

The scaling in SD conditions also depends on the type of problem. This behavior will be properly discussed later for each problem, but in all cases the results reveal a close relationship between the SD limit and the corresponding percolation problem: ordinary (isotropic) percolation for optimal paths [6,17,27–29,31–33] and undirected polymers [19,20], and directed percolation (DP) for directed polymers [25,26,34–37].

This paper is concerned with the crossover point between these two regimes, i.e., with the crossover scale below which those minimal paths behave as in the SD limit, and above which they behave as in WD. See, e.g., Refs. [28,29,31] for OPRL*s*, Refs. [17,31–33] for OPRN*s*, Refs. [25,26,34–37] for DPRM, and Ref. [20] for UPRM. This crossover also affects the properties of the global transport [10–12].

Indeed, as we will discuss more carefully later, much less is known on the scaling of the crossover point with disorder. Most of the results are for very specific and simple distributions and provide scaling laws that miss important information about the geometry and dimensionality of the network. In general, the approaches varied with the kind of problem but in all cases the crossover point was obtained from arguments based on the percolation theory. A notable exception is the work of Chen *et al.* [31]. The authors derived a model for the crossover length in the OPRL problem and for the crossover size in the OPRN problem. The models can be applied to any disorder distribution and they have shown to agree with the results of numerical simulations [17,18,28,29,31–33].

In this paper, we present a general theory for this crossover and show that it can be readily adapted to the three problems. Our argument is also based on the percolation theory, but we follow a different approach. Concretely, we focus on the role of the so-called red bonds of critical percolation in the behavior of those minimal paths in the SD limit. We recall that a red bond [38] is an open bond of a percolation lattice such that when it is removed, the connectivity inside the backbone of the percolation cluster to which it belongs is destroyed. Our results will also lead us to propose a universal measure of the disorder strength in these systems. That measure depends on both the disorder distribution and the percolation properties of the medium at criticality.

This paper is organized as follows. We begin by introducing in Sec. II some relevant concepts on the measure of disorder and presenting the families of distributions that will be used to generate it. Next, in Sec. III, we present our theoretical framework and derive the general scaling of the crossover length in the OPRL problem. This scaling will be studied numerically in Sec. IV, in which we also present an analytical expression based on a two-term approach. In Sec. V, we check the validity of our model by running numerical simulations of the OPRL problem. Once the OPRL problem has been understood, in Sec. VI we apply our reasoning to the OPRN, DPRM, and UPRM problems, in that order. In all cases, we will pay special attention to comparing our results to the different approaches followed in the literature. The last results of this paper will be presented in Sec. VII, where we propose and study a possible universal measure of the disorder strength. Finally, Sec. VIII is devoted to a summary of our conclusions and our ideas regarding future work.

II. ON DISORDER

We introduce the notion of *disorder strength* and assume that it can be measured through a certain parameter S, called the *disorder parameter*, which is obtained from the disorder distribution. To ensure that S provides a well-behaved measure, we impose the following conditions: (i) it is defined positive, (ii) it is a continuous and monotonic function of the distribution parameters, and (iii) the limit $S \to \infty$ corresponds to the SD limit and the limit $S \to 0$ is the WD limit, i.e., the homogeneous (nondisordered) case. The latter condition implies that the $S \to 0$ limit of $f(w)$ must be the Dirac delta $\delta(w - \tau)$, where τ is the expected weight of the distribution. One of the aims of this paper is to derive a universal expression for S, but for the moment we are interested in deducing a particular expression S_i for each type i of disorder.

In a previous work [30], we showed that the *coefficient of variation* (CV) of $f(w)$ provides a universal measure of the disorder strength in the OPRL problem on weakly disordered lattices. The CV of a distribution with mean τ and standard deviation s is $\text{CV} = s/\tau$. For $\text{CV} < 1$, there exists a length scale such that below it the optimal path behaves as in the WD limit, i.e., following the Gaussian statistics, and above it the optimal path behaves as in WD, i.e., following the KPZ statistics [30]. That crossover length scales as $(\text{CV})^{-2}$ and it diverges in the WD limit ($\text{CV} = 0$). At $\text{CV} = 1$ it becomes of the same order as the lattice constant and the effects of the lattice geometry seem to vanish [39]. In this paper, we are interested in the regime $\text{CV} \gg 1$, where we observe the effects of critical percolation [40]. Note that this regime is never achieved in distributions such as the uniform, in which CV is upper bounded by 1, or the exponential, with constant $\text{CV} = 1$.

Universal behavior is expected to be independent of the type of disorder. To check the universality of our results, we will consider the following families of distributions: the Weibull (W), the log normal (LN), the Pareto (P), the log Cauchy (LC), the inverse (I), and the polynomial (Poly). As we will see below, the identification of a disorder strength parameter in these families is straightforward. For that reason we

also address more complex distributions such as the Dagum (D) family, with two shape parameters.

We now present the density function of these families and our choice for the corresponding disorder parameter S_i. In all cases, there is a parameter, the scale or the location parameter depending on the distribution, which has been denoted by w_0. Since it is completely irrelevant for our purposes, we have considered $w_0 = 1$.

(i) The W family with support $[0, \infty)$ and shape parameter $k > 0$:

$$f_{\rm W}(w) = \frac{k}{w_0}\left(\frac{w}{w_0}\right)^{k-1} \exp\left[-\left(\frac{w}{w_0}\right)^{k}\right]. \tag{1}$$

The CV is a continuously decreasing function of k. Crossover value CV $= 1$ is obtained at $k = 1$, so we are interested in $k \ll 1$. Parameter $1/k$ agrees with all the requirements discussed above, so we define $S_{\rm W} \equiv 1/k$.

(ii) The LN family with support $[0, \infty)$ and parameter $\sigma > 0$:

$$f_{\rm LN}(w) = \frac{1}{w\sqrt{2\pi\sigma^2}} \exp\left[-\frac{\ln^2(w/w_0)}{2\sigma^2}\right]. \tag{2}$$

The CV is a continuously increasing function of σ. Crossover value CV $= 1$ is obtained at $\sigma \simeq 0.83$, so we will focus on values $\sigma \gg 1$. For the log normal distribution, we define $S_{\rm LN} \equiv \sigma$.

(iii) The P family with support $[w_0, \infty)$ and shape parameter $b > 0$:

$$f_{\rm P}(w) = \frac{b}{w_0}\left(\frac{w_0}{w}\right)^{b+1}. \tag{3}$$

The CV is well-defined only for $b > 2$ and is a continuously decreasing function of b. Crossover value CV $= 1$ is obtained at $b \simeq 2.41$, so we will be interested in values $b \ll 1$. Accordingly, for the Pareto distribution, we define $S_{\rm P} \equiv 1/b$.

(iv) The LC family with support $[0, \infty)$ and parameter $\gamma > 0$:

$$f_{\rm LC}(w) = \frac{1}{w\pi}\left[\frac{\gamma}{\ln^2(w/w_0) + \gamma^2}\right]. \tag{4}$$

The CV of the log Cauchy is not defined because its mean and variance are infinite. However, simulation results lead us to define $S_{\rm LC} \equiv \gamma$ and focus on $\gamma \gg 1$.

(v) The I family with support $[1, e^a]$ and parameter $a > 0$:

$$f_{\rm I}(w) = \frac{1}{aw}. \tag{5}$$

The CV is a continuously increasing function of a, which clearly controls the broadness of the disorder. Crossover value CV $= 1$ is obtained at $a = 3.83$. Thus, we define $S_{\rm I} \equiv a$ and SD conditions are expected for $a \gg 1$.

(vi) The Poly family with support [0,1] and exponent $\alpha > 0$, called the *extreme value index* [10–12]:

$$f_{\rm Poly}(w) = \alpha w^{\alpha-1}. \tag{6}$$

This family has the particularity that its distribution function $F_{\rm Poly}(w) = w^{\alpha}$ shows a power-law behavior close to zero which is different from the linear behavior of regular distributions around zero [12]. The CV is a continuously decreasing function of α, which controls the disorder strength. The SD and WD limits are obtained when $\alpha \to 0$ and $\alpha \to \infty$, respectively [12]. Crossover value CV $= 1$ is obtained at $\alpha \simeq 0.414$, so SD conditions are expected for $\alpha \ll 1$. We define $S_{\rm Poly} \equiv 1/\alpha$.

(vii) The D family with support $[0, \infty)$ and two shape parameters, β and χ;

$$f_{\rm D}(w) = \frac{\beta\chi}{w}\frac{(w/w_0)^{\beta\chi}}{(1 + (w/w_0)^{\chi})^{\beta+1}}. \tag{7}$$

The CV of the Dagum distribution is not defined for $\chi \leqslant 2$ because the variance diverges. For fixed β, it is a decreasing function of χ with $\lim_{\chi\to\infty}$ CV $= 0$. For fixed χ, it is a decreasing function of β with the following limits: $\lim_{\beta\to 0}$ CV $= \infty$ and $\lim_{\beta\to\infty}$ CV $= K(\chi)$, where $K(\chi)$ is a positive decreasing function of χ with $\lim_{\chi\to\infty} K(\chi) = 0$. Therefore, the WD limit can only be reached in the $\chi \to \infty$ limit. On the other hand, the SD limit can be attained when $\beta \to 0$ or $\chi \to 0$. This is a very interesting case since the SD limit can be achieved through two distribution parameters, so it is not so obvious defining the Dagum disorder parameter $S_{\rm D}$. For the moment, we choose $S_{\rm D} \equiv (\beta\chi)^{-1}$. A deeper analysis of this question will be presented in Sec. VII.

We summarize in Table I our choice for the disorder strength parameter S_i of each family i of distributions. We recall that, in all cases, the SD regime is observed for $S_i \gg 1$ and the SD limit is obtained when $S_i \to \infty$.

TABLE I. Disorder strength parameter S_i of each family i of distributions.

i	W	LN	P	LC	I	Poly	D
S_i	k^{-1}	σ	b^{-1}	γ	a	α^{-1}	$(\beta\chi)^{-1}$

III. THEORETICAL CONSIDERATIONS (OPTIMAL PATHS)

In this section, we present our theoretical arguments and several numerical results supporting them. We do it for the OPRL problem [17,18,23,27–29,31–33,41]. In further sections, we adapt them to the OPRN, DPRM, and UPRM problems. More specifically, we consider the problem of the optimal path between two opposite sides of a square lattice of linear size L, although our arguments and results are also valid for the problem of the optimal path between two fixed points in a lattice [18].

Before starting, we introduce an object that will be very useful throughout the paper to present our theory. Given a disordered lattice, for a certain value of the weight w' we define the *corresponding percolation lattice* CPL(w') as the bond percolation lattice obtained from the initial disordered lattice when we consider that all bonds with weights $w \leqslant w'$ are open bonds and all bonds with $w > w'$ are closed. The occupation probability of the CPL(w') is thus $p = F(w')$.

OPRLs in the SD limit are self-similar objects that belong to the same universality class as paths in the minimum spanning tree [4,10–12] and shortest paths in invasion percolation with trapping [5,6]. Much evidence points to a close

relationship between OPRL*s* in the SD limit and ordinary bond percolation at criticality [6,17,27–29,31–33]. Indeed, the so-called *bombing algorithm* proposed by Cieplak *et al.* [27] to obtain the optimal path in the SD limit is actually a percolation process.

It is also clear that the optimal path in the SD limit, with total weight $W_{\rm opt} = w_{\rm max}$, belongs to the backbone of the percolation cluster obtained in the CPL($w_{\rm max}$). Moreover, this is the cluster that (for the first time) percolates the lattice. This means that clusters obtained in CPL($w < w_{\rm max}$) are not percolating.

The relationship between OPRL*s* in the SD limit and percolation is well established by the relation $p = F(w)$, which represents a continuous mapping of the weight into the occupation probability of the percolation problem [40]. We have recently shown [40] that the *optimal balls* $B(W)$, given by the set of nodes that can be reached from the center node by optimal paths with weight $W_{\rm opt} \leqslant W$, are, in the SD limit, statistically equal to the percolation clusters obtained at occupation probability $p = F(W)$. For weakly disordered lattices the fluctuations of the optimal balls obey KPZ statistics [39].

From these results, we deduce that the probability density of $w_{\rm max}$ in the SD limit, denoted as $\rho'(w_{\rm max}, L)$, has the form

$$\rho'(w_{\rm max}, L) = f(w_{\rm max})\rho(p, L), \tag{8}$$

where $\rho(p, L)$ is the probability density for a percolation cluster to span a square lattice of side L with occupancy p. For $L \to \infty$, we have the following asymptotic behaviors [38,42]: (i) $\rho(p_c, L) \sim L^{1/\nu}$, where ν is the percolation exponent associated to the scaling of the *correlation length* ξ near criticality, $\xi \sim |p_c - p|^{-\nu}$, which is well-defined for any dimension $\mathcal{D}$; (ii) the standard deviation of $\rho(p, L)$ decreases as $L^{-1/\nu}$, and (iii) the probability that the lattice percolates at probability p_c, given by the function $\Pi(p_c, L) = \int^{p_c} \rho(p', L)dp'$, approaches $1/2$ in site percolation and is equal to $1/2$ for all L in bond percolation.

By applying these results to Eq. (8), we obtain that the $L \to \infty$ limit of $w_{\rm max}$ is the *critical weight*:

$$w_c \equiv F^{-1}(p_c). \tag{9}$$

For finite L, $w_{\rm max}$ is distributed around w_c [28,29] with a standard deviation that scales as $L^{-1/\nu}$ [28].

We now apply to our OPRL problem the *links-nodes-blobs* picture proposed by Stanley to describe the infinite cluster slightly above criticality [43]. According to that picture, the backbone of the bond percolation cluster that connects for the first time the left and the right sides of a percolation square lattice of linear size $L < \xi$ can be represented schematically as shown in Fig. 1. The backbone behaves as a generalized link between the two sides consisting of a series of *blobs* (gray regions) connected by one-dimensional chains of *red bonds* (thick lines). We recall that the backbone of a percolation cluster carries all the current flowing through the cluster if we impose a voltage drop between the two opposite plates. The red bonds (also called *singly connected bonds*) are those links of the backbone which carry the full current [38,43,44]. When a red bond is removed, the current between the two plates stops because the connectivity between them is destroyed. Finally, the blobs are sets of multiconnected bonds left after removing the red bonds from the backbone. Blobs are dense regions with more than one connection between two nodes.

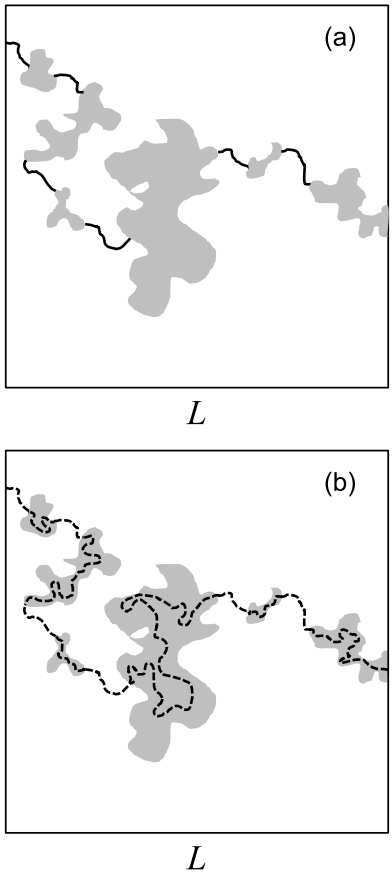

FIG. 1. (a) Schematic picture for the backbone of the percolation cluster that, for the first time, connects the left and the right sides of a square lattice. We have followed the links-nodes-blobs picture [43]. One-dimensional chains of red bonds are represented by thick lines and blobs by gray regions. (b) Illustration of the optimal path (broken line) between the two opposite sides.

It seems clear that the optimal path between the two opposite sides in the SD limit must go through all the red bonds in the backbone of the percolation cluster obtained in the CPL($w_{\rm max}$). We have illustrated this idea in Fig. 1(b), in which we have schematically represented the optimal path between the two sides by the broken curve. This path must traverse all the singly connected segments since they act as bottle necks. When the path reaches a blob, it explores the entire patch to minimize the weight between the entry and the exit blob points.

The average number of red bonds in a percolation lattice of linear size $L < \xi$, denoted by $n_{\rm red}$, scales as [44]

$$n_{\rm red} \sim L^{1/\nu}. \tag{10}$$

We have carried out numerical simulations of the OPRL problem in square lattices of linear size L and we have measured $n_{\rm red}$ as follows. For each optimal path, we first identify $w_{\rm max}$ and then we build the CPL($w_{\rm max}$). Finally, we calculate the number of red bonds in the backbone of the resulting percolation cluster. We show in Fig. 2(a) the results obtained for a Weibull disorder with different disorder strengths. We

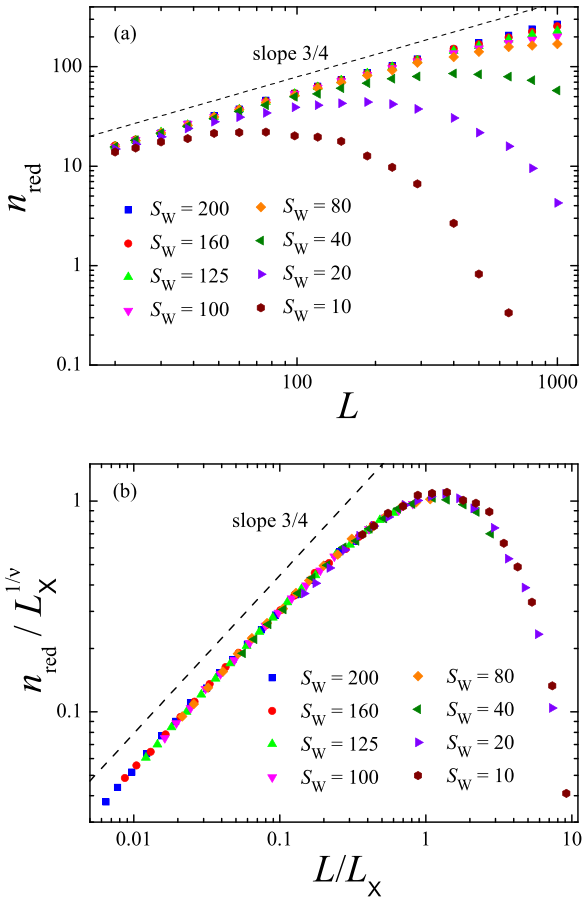

FIG. 2. (a) Average number of red bonds in the optimal path between two opposite sides of a square lattice as a function of the lattice linear size L for a Weibull disorder with different values of S_W. (b) Data collapse obtained after scaling L to the SD-WD crossover length $L_\times$ given in Eq. (23), and n_{red} to $L_\times^{1/\nu}$. Dashed line in both panels represents power-law behavior with exponent $1/\nu = 3/4$. Averages are calculated over 5000 realizations.

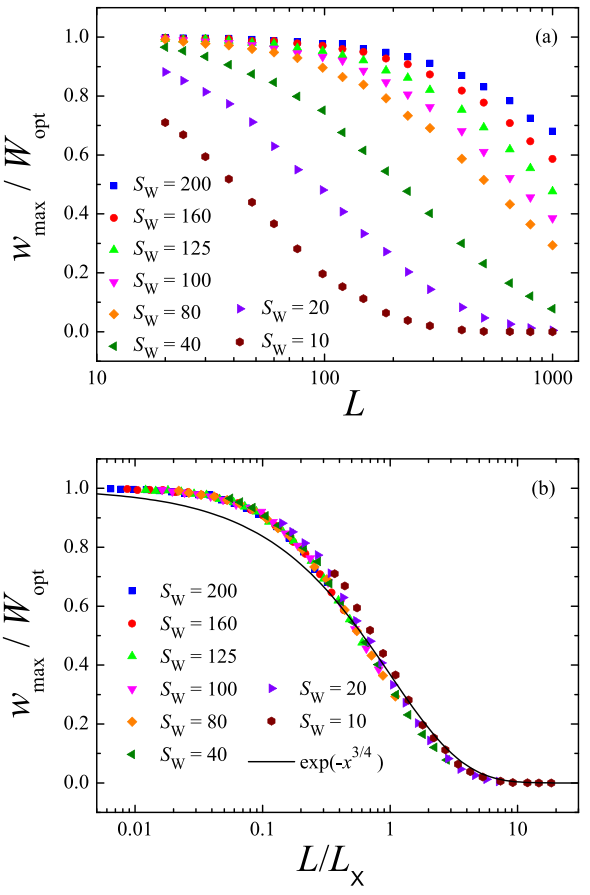

FIG. 3. (a) Ratio w_{max}/W_{opt} as a function of the lattice linear size L for the same set of results displayed in Fig. 2. (b) Data collapse obtained after scaling L to the SD-WD crossover length $L_\times$ given in Eq. (23). Continuous line represents function $w_{max}/W_{opt} = \exp(-x^{3/4})$ with $x \equiv L/L_\times$, deduced after applying the theoretical arguments presented in Ref. [25] to the OPRL problem (see Sec. VI B). Averages are calculated over 5000 realizations.

clearly see that the curves follow the scaling behavior given in Eq. (10) up to a certain point that depends on the disorder strength. As S_W increases, the deviation takes place in increasingly larger lattices.

That deviation occurs when the max principle is no longer fulfilled and the optimal path departs from the SD limit behavior. To illustrate it, we have displayed in Fig. 3(a) the ratio w_{max}/W_{opt} for the same set of simulations. As disorder strength increases, the range of validity of the max principle ($w_{max}/W_{opt} = 1$) also increases. In the SD limit ($S_W \to \infty$), this range should extend to infinite.

When we compare Figs. 2(a) and 3(a), we note that the deviations from the SD limit behavior take place in both cases at similar points. We denote this crossover length as $L_\times$. Thus, $L_\times$ stands for the length scale above which the max principle is no longer fulfilled and the system deviates from the SD limit behavior. We expect it to depend on the disorder distribution and on the geometric and topological properties of the lattice. From the results displayed in the figures, we also deduce that it is an increasing function of disorder. We anticipate that the data collapses displayed in the panels below, Figs. 2(b) and 3(b), support this assumption.

Continuing with our reasoning, it is also reasonable to assume that the bond with the largest weight w_{max} must be a red bond. Otherwise, it would belong to a blob and hence it would be discarded in the optimization process. To validate this assumption, we have calculated the probability for it to occur, denoted as P_{red}, in the same set of results presented above. Results have been displayed in Fig. 4(a). The similarity with Fig. 3(a) is very remarkable and clearly shows that, as long as the problem behaves as in the SD limit, the probability is practically one.

Suppose now that we are at some point in the crossover region from SD to WD, so the max principle does not strictly hold. We can thus assume that the total weight of the optimal path is controlled by the sum of the weights of the red bonds along the path:

$$W_{opt} \approx \sum_{k=1}^{n_{red}} w_k. \tag{11}$$

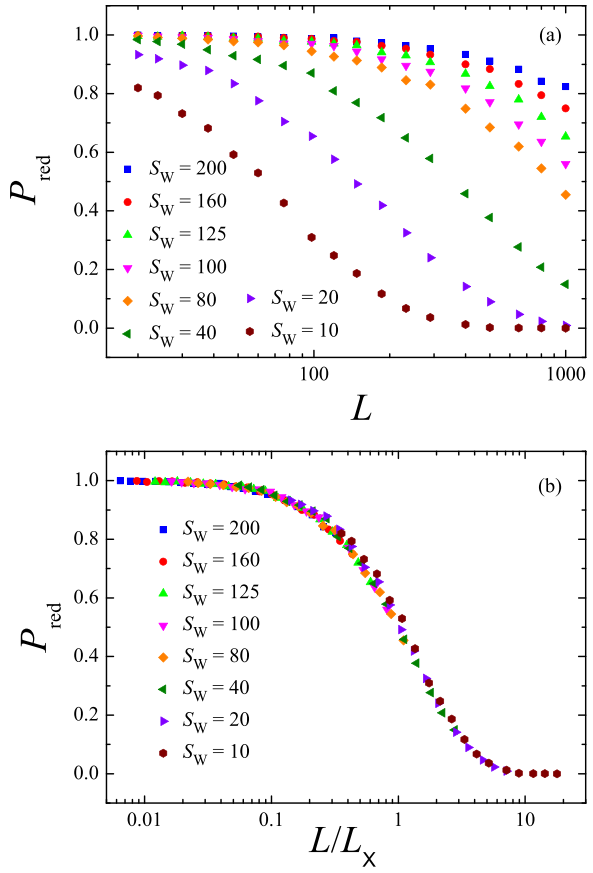

FIG. 4. (a) Probability that the bond with w_{max} is a red bond as a function of the lattice linear size L for the same set of results displayed in Figs. 2 and 3. (b) Data collapse obtained after scaling L to the SD-WD crossover length $L_\times$ given in Eq. (23). Averages are calculated over 5000 realizations.

That assumption is reasonable since the same argument used to show that the maximal bond must be a red bond can be applied to the second heaviest bond, to the third, and so on until we get bond weights comparable to the blobs weights. Indeed, close to the crossover one expects that only the highest valued bonds along the paths are relevant [26]. However, as we will show later, it is enough considering the first two terms, which is in line with the approaches followed in the literature [20,25,26,28,31,32].

The weights of the red bonds are assumed to be i.i.d. random variables because their choice obeys a geometrical principle (conservation of connectivity) instead of a minimal principle. In the SD limit and for large L, the probability density and cumulative distribution of the red-bond weights, denoted by f_{red} and F_{red}, respectively, are

$$f_{red}(w) = \frac{f(w)}{p_c}, \quad F_{red}(w) = \frac{F(w)}{p_c}, \tag{12}$$

with support $[w_A, w_c]$.

From the above arguments and Eq. (10), we conclude that the problem of obtaining the crossover length $L_\times$ can be simplified to the problem of determining the length of a one-dimensional chain of i.i.d. random variables at which the max principle fails. We denote this crossover number by $n^\times_{red}$ and we obtain

$$L_\times \sim (n^\times_{red})^\nu. \tag{13}$$

The crossover length $L_\times$ depends on the properties of the disorder distribution and the geometry and dimensionality of the lattice through p_c and ν.

IV. CHAIN MODEL

To obtain the SD-WD crossover number $n^\times_{red}$, we must set the mathematical condition for the transition to occur.

We consider a chain of $n+1$ bonds and assume that the bond at position $n+1$ has the critical weight w_c. The rest of the bonds have random weights w_i drawn from the probability density f_{red} given in Eq. (12) with $w \in [w_A, w_c]$. Now, we look for the probability that the total weight of the rest of the chain, $\sum_{i=1}^n w_i$, is less than w_c [12]. We define that probability as

$$\mathbf{P}(n, S) \equiv \text{Prob}\left\{\sum_{i=1}^{n} w_i < w_c : w_i < w_c\right\}. \tag{14}$$

$\mathbf{P}(n, S)$ is, in fact, the cumulative distribution of the n convolution of $f_{red}(w)$, evaluated at w_c.

For $n \ll n^\times_{red}$, the chain should behave as in the SD limit, hence giving $\mathbf{P}(n, S) \simeq 1$. For $n \gg n^\times_{red}$, the chain is weakly disordered and we should obtain $\mathbf{P}(n, S) \simeq 0$. We thus expect

$$\mathbf{P}(n, S) \simeq \begin{cases} 1 & \text{for } n \ll n^\times_{red} \\ 0 & \text{for } n \gg n^\times_{red}. \end{cases} \tag{15}$$

To check this conjecture, we have numerically calculated $\mathbf{P}(n, S)$ and we have displayed the results in Fig. 5. Figure 5(a) shows $\mathbf{P}(n, S)$ against n for different strengths of the Weibull disorder. In Fig. 5(b), we show the results for several families of distributions with the same strength $S_i = 1000$.

We first note that the decay of $\mathbf{P}(n, S)$ with n follows the behavior conjectured in Eq. (15). Moreover, this decay is in excellent agreement with the stretched exponential function,

$$\mathbf{P}(n, S) \approx \exp\left[-\left(\frac{n-1}{n^\times_{red}-1}\right)^\phi\right], \tag{16}$$

with parameters $n^\times_{red} > 1$ and $\phi > 0$. From the definition of $\mathbf{P}$, we have $\mathbf{P}(1, S) = 1$ regardless of the disorder strength S. Data fits to Eq. (16) have been represented by continuous lines of the same color as the corresponding symbols. It is important to stress that we have obtained the same excellent agreement in all the families studied in this work. Thus, the behavior presented in Eq. (16) seems to be universal.

In Fig. 5(a), we observe that $\mathbf{P}(n, S_W \to \infty) \to 1$ for all n, which means that $n^\times_{red}$ diverges in the SD limit, as expected. In Fig. 5(b), we also observe that disorder parameters S_i do not provide a universal measure of the disorder strength. Otherwise, data would collapse to a single universal function. We focus now on the fitting parameters $n^\times_{red}$ and ϕ. We show their fitted values in Figs. 6(a) and 6(b), respectively, as a function of the disorder parameter S_i for several families of distributions. We observe that $n^\times_{red}$ very rapidly attains its asymptotic behavior, which seems to be linear in all cases.

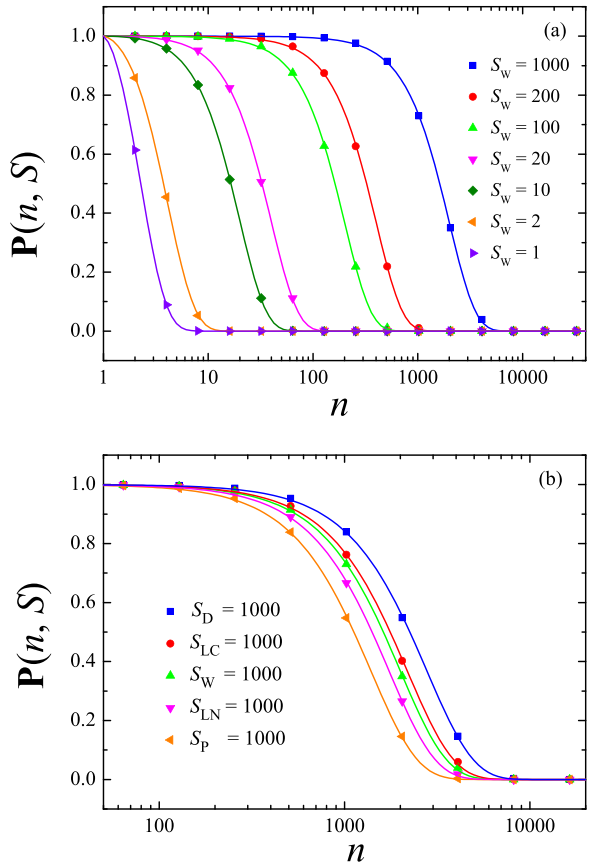

FIG. 5. Numerical estimate of probability $\mathbf{P}(n, S)$ as a function of n for (a) the Weibull distribution and different values of its disorder parameter S_W and (b) different families of distributions with the same disorder strength $S_i = 1000$. To obtain the Dagum set of points, we have fixed $\beta = 1$ and varied χ. The fit of each set of symbols to the stretched exponential function given in Eq. (16) has been displayed in both panels with continuous lines of the same color. Probabilities are calculated from 10^6 simulations of the chain model.

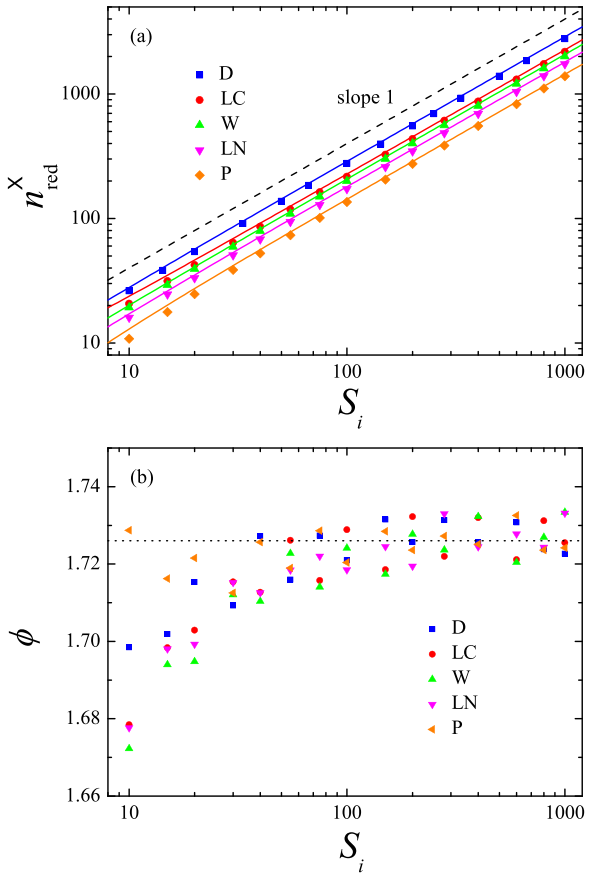

FIG. 6. (a) Crossover number of red bonds, $n^{\times}_{red}$, obtained from the fit of $\mathbf{P}(n, S)$ to the stretched exponential function given in Eq. (16) as a function of the corresponding disorder parameter S_i for several families of distributions. Continuous lines with the same color as the symbols stand for the analytical approximate given in Eq. (20). The broken line represents linear behavior. (b) Fitted values of the stretching exponent ϕ as a function of S_i for the same results. Dotted line represents the value $\phi = 1.726$ (see text).

The stretching exponent approaches a limit value that, interestingly, seems to be universal as well. We have fitted $n^{\times}_{red}$ to the power law $c_i(S_i)^{m_i}$ for values $S_i > 100$, and the results are shown in Table II. Indeed, the fitted value of the exponent m_i is practically equal to 1 in all the cases.

It is worth noting that this result depends on our choice of the disorder parameter for each family, S_i, which was given in Table I. For example, for the Weibull family we could also have considered $S_W = k^{-q}$ with $q > 0$, since it satisfies all the conditions we have imposed. That case would appear in the figure as a straight line with slope $1/q$. Definitions given in Table I were intended to show that in all the families analyzed here there exists a definition of disorder parameter such that $n^{\times}_{red}$ grows linearly with it, and that this definition is closely related to the shape parameter of the corresponding family. Furthermore, we will see later that this choice corresponds to the asymptotic behavior of our theoretical model.

We also display in the table, for each family i, the value ϕ_i obtained from direct averaging of the values of ϕ displayed

TABLE II. For each family i, the first two rows show the values of the fitting parameters c_i and m_i resulting from the fit of $n^{\times}_{red}$ in Fig. 6(a) to function $c_i(S_i)^{m_i}$ for $S_i > 100$. The third row shows the value ϕ_i obtained from direct averaging of the values of ϕ displayed in Fig. 6(b) for $S_i > 100$. The bottom row shows the prefactor C_i in the asymptotic behavior of $n^{\times}_{red}$ given in Eq. (21).

i	Weibull	Log normal	Pareto	Log Cauchy	Dagum
c_i	2.01 ± 0.01	1.707 ± 0.006	1.329 ± 0.005	2.162 ± 0.008	2.73 ± 0.02
m_i	1.000 ± 0.001	1.0027 ± 0.0005	1.0062 ± 0.0006	1.0012 ± 0.0006	1.003 ± 0.001
ϕ_i	1.726 ± 0.002	1.727 ± 0.001	1.726 ± 0.001	1.726 ± 0.002	1.728 ± 0.002
C_i	$\frac{1}{\ln^2 2} \simeq 2.08$	$\frac{\sqrt{\pi/2}}{\ln 2} \simeq 1.81$	$\frac{1}{\ln 2} \simeq 1.44$	$\frac{\pi}{2 \ln 2} \simeq 2.27$	$\frac{2}{\ln 2} \simeq 2.89$

in Fig. 6(b) for $S_i > 100$. The SD limit of the stretching exponent is very close to 1.726. The apparent universality of this value is certainly striking. It points to a universal mathematical property of the SD limit which emerges when the set of weights becomes ultrametric. Although it is indeed a very interesting issue, it is not relevant for our purposes and we have not addressed it.

A. Analytical two-term approach

We can obtain an analytical estimate of $n^{\times}_{\rm red}$ if we simplify the problem to a two-term approach. We consider again a chain of $n+1$ bonds in which one of the bonds has a weight w_c. However, we suppose now that the rest of the bonds are only of two types: bonds with weights $w_i < w_c/2$, which we suppose negligible, and bonds with weights in the interval $w_i \in [w_c/2, w_c]$, called heavy bonds. The probability of having a negligible bond is

$$\mathcal{P} \equiv F_{\rm red}(w_c/2) = \frac{F(w_c/2)}{p_c}, \tag{17}$$

and of having a heavy bond is $1-\mathcal{P}$.

To calculate the probability $\mathbf{P}(n,S)$ that the total weight of the rest of the chain is less that w_c, we must take into account that only one heavy bond is allowed. We then have

$$\mathbf{P}(n,S) = \mathcal{P}^n + n\mathcal{P}^{n-1}(1-\mathcal{P}). \tag{18}$$

Notice that a different cutoff weight of the form w_c/N, with $N>2$, would involve more terms, so this is the simplest approach. Now we can write the above expression in the form

$$\mathbf{P}(n,S) = \mathcal{P}^n\left(1+\frac{n}{n^{\times}_{\rm red}}\right), \tag{19}$$

with

$$n^{\times}_{\rm red} = \frac{\mathcal{P}}{1-\mathcal{P}}. \tag{20}$$

The argument that supports this definition of the crossover number $n^{\times}_{\rm red}$ is the following. In all the families addressed here, we have found $(1-\mathcal{P}) \sim S_i^{-1}$ as we approach the SD limit. In that limit, we then have $\mathcal{P}=1$. For $n \ll n^{\times}_{\rm red}$, Eq. (19) has the form $\mathbf{P}(n,S) \approx \mathcal{P}^n$. This expression accounts for the case in which the rest of the bonds are all negligible, which is the definition of the max principle. Thus, term $\mathcal{P}^n$ stands for the asymptotic behavior of $\mathbf{P}$ as we approach the SD limit. We hence conclude that $\mathbf{P}(n,S) \simeq 1$ for $n \ll n^{\times}_{\rm red}$. On the other hand, for $n \gg n^{\times}_{\rm red}$ we obtain $\mathbf{P}(n,S) \approx n\mathcal{P}^{n-1}(1-\mathcal{P})$. This expression accounts for the case in which we have *at least* one bond with a weight comparable to $w_{\rm max}$, which is the definition of the WD regime. Notice that $\mathbf{P}$ is proportional to the length n of the chain. We thus conclude that $\mathbf{P}(n,S) \simeq 0$ for $n \gg n^{\times}_{\rm red}$. Therefore, the definition of $n^{\times}_{\rm red}$ given Eq. in (20) is consistent with the overall behavior depicted in Eq. (15). We also deduce that $n^{\times}_{\rm red}$ behaves asymptotically in the form

$$n^{\times}_{\rm red} = C_i S_i + O(1) \quad \text{as} \quad S \to \infty, \tag{21}$$

which is in agreement with the results displayed in Fig. 6(a) and Table II.

To check our analytical approach, we have displayed in Fig. 6(a) with continuous lines the values of $n^{\times}_{\rm red}$ obtained from Eq. (20). The agreement with the numerical results of the complete chain model is quite remarkable. We have also deduced the prefactors C_i in the above asymptotic behavior. Their exact expressions and approximate values are shown in Table II for each type of disorder. We can now compare these values to the values of c_i obtained in the complete chain model (second row in the table). The agreement is reasonably good and the largest difference is about 8%. In all cases, the c_i are slightly smaller than the C_i. This is an expected result since the contribution of all the bonds in the chain makes the crossover occur at smaller values of $n^{\times}_{\rm red}$.

Finally, from Eq. (13) we obtain the scaling of the crossover length $L_\times$ in the OPRL problem,

$$L_\times \sim \left(\frac{\mathcal{P}}{1-\mathcal{P}}\right)^{\nu} \quad \text{(OPRL)}, \tag{22}$$

which is a functional of the *disorder function* $n^{\times}_{\rm red} = \mathcal{P}/(1-\mathcal{P})$.

V. RESULTS AND DISCUSSION

In Figs. 2(a), 3(a), and 4(a), we have shown how different observables deviate at a certain point from the SD limit behavior. In Figs. 2(b), 3(b), and 4(b) we have represented the same results but L has been scaled to the crossover length $L_\times$ given in Eq. (22), which for the Weibull family takes the form

$$(L_\times)_{\rm W} \sim \left[\frac{1-(1-p_c)^{2^{-k}}}{p_c-1+(1-p_c)^{2^{-k}}}\right]^{\nu}. \tag{23}$$

In Fig. 2, we have also scaled the average number of red bonds to its value at the crossover point, $n^{\times}_{\rm red} \sim L_\times^{1/\nu}$.

In the three cases, our model yields an excellent collapse of data to a single curve. Very small deviations appear only for the weakest disorder $S_{\rm W}=10$. Moreover, the transition point in each curve seems to be very close to the value $L/L_\times = 1$, which indicates that the prefactor in the scaling law of $L_\times$ given in Eq. (22) is of the order of unity.

Our model for the crossover length also successfully accounts for the SD-WD transition of other relevant observables such as the length of the optimal path, $\ell_{\rm opt}$. We have calculated the average length of the optimal path between points A and B located at positions $(-r/2,0,0)$ and $(r/2,0,0)$, respectively, in cubic lattices of linear size $L \geqslant r$ with corners located at positions $(\pm L/2, \pm L/2, \pm L/2)$. The end-to-end distance r is fixed to $r=10$. Results are displayed in Fig. 7 as a function of the lattice size L for different strengths of the Weibull disorder. The nice collapse displayed in the figure is obtained when L is scaled to $L_\times$ and $\ell_{\rm opt}$ to $L_\times^{\kappa/\nu-\varphi}$ with $\varphi = 0.53$ and $\kappa = 1.25$ (see Ref. [18] for more details).

We now discuss the relation between our model for $L_\times$ and the approaches followed in the literature [28,29,31]. As mentioned before, these approaches focus on the two largest weights along the path, the maximal weight $w_{\rm max}$ and the second largest weight, say w_2. When w_2 becomes of the same order as $w_{\rm max}$, we no longer have a single bond dominating the optimal path and the transition takes place. We can now apply the percolation theory and assume that w_2 gets closer to $w_{\rm max}$ in the same way that $w_{\rm max}$ gets closer to w_c, i.e., as $\sim L^{-1/\nu}$. Applying this reasoning to the inverse distribution, we obtain

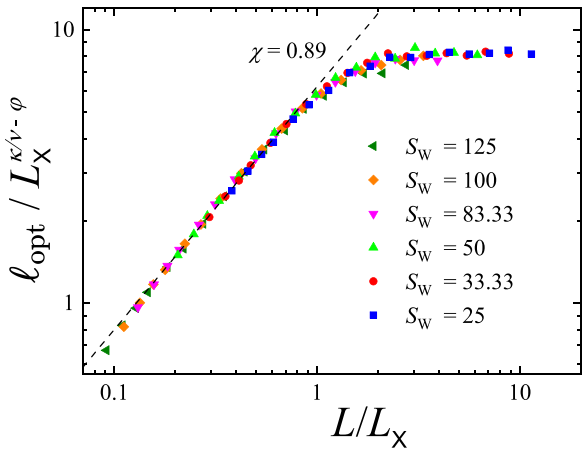

FIG. 7. Scaled average optimal path length $\ell_{\rm opt}/L_\times^{\kappa/\nu-\varphi}$ as a function of scaled linear size $L/L_\times$ for different Weibull-disorder strengths. $L_\times$ is calculated from the expression given in Eq. (23). We study the optimal path between two points on the axis separated by an end-to-end distance $r = 10$ in simple cubic lattices of linear size $L > r$. Averages are calculated over 5000 realizations.

that $L_\times$ scales with the disorder strength a as $L_\times \sim a^\nu$ [28,29]. On the other hand, from Eq. (22) we obtain

$$(L_\times)_{\rm I} \sim \left(\frac{ap_c}{\ln 2} - 1\right)^\nu, \tag{24}$$

which agrees asymptotically with that finding, but which also shows that the crossover length scales with the geometry and dimensionality of the lattice through the critical probability p_c.

Chen *et al.* [31] derived the general expression $L_\times \sim A^\nu$, where A is the disorder function:

$$A = \frac{p_c}{w_c f(w_c)}. \tag{25}$$

This model was found in agreement with the simulations [31] and it has been recently used to derive a unified scaling for the optimal path length in the OPRL problem [18]. For the inverse distribution, their model gives $L_\times \sim (ap_c)^\nu$, which is quite similar to our result in Eq. (24).

That similarity is due to the simplicity of the inverse distribution, but the remarkable point is that $n_{\rm red}^\times$ and A have the same asymptotic behavior as we approach the SD limit ($S \to \infty$). For $\mathcal{P}$ close to 1, Eq. (20) behaves as

$$n_{\rm red}^\times \simeq \frac{1}{1-\mathcal{P}} = \frac{p_c}{\int_{w_c/2}^{w_c} f(w)dw}. \tag{26}$$

In that vicinity, we also have $\int_{w_c/2}^{wc} f(w)dw \sim w_c f(w_c)$, hence obtaining $n_{\rm red}^\times \sim A$. More specifically, for all the distributions addressed here, we have found

$$n_{\rm red}^\times = (\ln 2)^{-1} A + \mathcal{O}(1) \quad \text{as} \quad S \to \infty. \tag{27}$$

VI. APPLICATIONS

In this section, we adapt our theory to the OPRN, DPRM, and UPRM problems, in that order.

A. Random networks

Optimal paths in disordered random networks also undergo a transition from strong to weak disorder [4,10–12,17,31–33,45]. The most studied random graphs are the Erdős-Rényi (ER) and the *scale-free* (SF) networks. For WD, the average length of the optimal path between two nodes in the network of N nodes scales as $\ell_{\rm opt} \sim \log N$ [17,45] for both ER and SF networks. In the SD regime, for ER networks we have $\ell_{\rm opt} \sim N^{1/3}$ [17,45] whereas for SF networks the behavior depends on the distribution of the node degree g, $P(g) \sim g^{-\lambda}$: for $3 < \lambda < 4$, we have $\ell_{\rm opt} \sim N^{(\lambda-3)/(\lambda-1)}$, for $\lambda \geqslant 4$ we have $\ell_{\rm opt} \sim N^{1/3}$, and for the case $2 < \lambda < 3$ it has been suggested that $\ell_{\rm opt} \sim \ln^{\lambda-1} N$ [17]. However, this case is rather irrelevant to us because it possesses only a percolative phase [46].

To deduce the crossover network size at which the SD-WD crossover takes place, denoted as $N_\times$, we will also make use of the fact that the SD limit of these systems is closely related to their corresponding critical percolation [17,45]. Indeed, the SD limit behaviors presented above can be deduced using percolation arguments [17,41].

We assume that percolation on random networks at criticality is equivalent to critical percolation on regular lattices in a certain dimension $\mathcal{D}$ [17,45,46]. Using the equivalence relation $N_\times \sim L_\times^{\mathcal{D}}$ in Eq. (13), we obtain

$$N_\times \sim (n_{\rm red}^\times)^{\mathcal{D}\nu}. \tag{28}$$

Erdős-Rényi networks are equivalent, at criticality, to critical percolation regular lattices at the upper critical dimension $\mathcal{D}_c = 6$ [17,45]. In $\mathcal{D} = 6$, we have $\nu = 1/2$ [38] and we obtain

$$N_\times \sim \left(\frac{\mathcal{P}}{1-\mathcal{P}}\right)^3 \quad \text{(ER)}. \tag{29}$$

For SF networks with $3 < \lambda < 4$, we have $\mathcal{D} = 2(\lambda - 1)/(\lambda - 3)$ [46]. Since $\mathcal{D} > \mathcal{D}_c$, we must consider $\nu = 1/2$ and we obtain

$$N_\times \sim \left(\frac{\mathcal{P}}{1-\mathcal{P}}\right)^{(\lambda-1)/(\lambda-3)} \quad \text{(SF with } 3 < \lambda < 4\text{)}. \tag{30}$$

For SF networks with $\lambda > 4$, we have $\mathcal{D} = \mathcal{D}_c = 6$ [46] and $\nu = 1/2$, and we obtain

$$N_\times \sim \left(\frac{\mathcal{P}}{1-\mathcal{P}}\right)^3 \quad \text{(SF with } \lambda > 4\text{)}. \tag{31}$$

These results are in perfect agreement with the results of Chen *et al.* [31]. We recall that our disorder function $n_{\rm red}^\times = \mathcal{P}/(1-\mathcal{P})$ behaves asymptotically as their disorder function A [see discussion in Sec. V and Eq. (27)]. These scaling laws have been verified by numerical simulations. See, e.g., Ref. [31] for different types of disorder and Refs. [17,32,33] for the inverse distribution.

The polynomial distribution was used in Refs. [10–12] for ER graphs and square lattices. In Ref. [11], the authors reported a phase transition in the properties of the overall transport at a critical extreme value index α_c. For a network of size N, for $\alpha \gg \alpha_c$ we have WD conditions and the transport traverses many links. For $\alpha \ll \alpha_c$, the transport behaves as in the SD limit and thus follows the *minimum spanning tree*.

Numerical simulations showed that $\alpha_c \propto N^{-\beta}$ with $\beta \approx 0.63$ for ER graphs and $\beta \approx 0.62$ for square lattices.

For the polynomial distribution in Erdős-Rényi graphs, our model gives

$$(N_\times)_{\text{Poly}} \sim (2^\alpha - 1)^{-3}. \tag{32}$$

We now apply the conditions in Ref. [11]. For a network of size N we calculate the value of α, say $\alpha_\times$, that makes the crossover size $N_\times$ of the same order as the network size N. From Eq. (32), we obtain

$$\alpha_\times \sim \ln(1 + N^{-1/3}) \sim N^{-1/3} \quad \text{as} \quad N \to \infty. \tag{33}$$

Doing the same for square lattices with $N = L^2$, we obtain

$$\alpha_\times \sim N^{-1/2\nu} = N^{-3/8} \quad \text{as} \quad N \to \infty. \tag{34}$$

Our scaling exponents for $\alpha_\times$ clearly differ from the scaling exponents of α_c deduced from their numerical simulations. This disagreement might be due to the fact that Eqs. (33) and (34) account for the asymptotic behavior, while the results in Ref. [11] were obtained for relatively small networks, for which we can expect contributions from highest order terms such as the term $N^{-2/3}$ in Eq. (33). Certainly, this question needs further investigation and clarification.

B. Directed polymers

Directed polymers in WD belong to the KPZ universality class, while their SD limit seems to belong to the DP universality class [25,26,34–37]. As in the isotropic case, the transition from SD to WD takes place when the max principle is no longer fulfilled [25,26].

Evidence of the close relationship between the SD limit of DPRM and directed percolation is the roughness exponent ζ. It characterizes the scaling of the transverse displacement of the optimal directed polymer, $|\mathbf{x}|$, with its length t, $|\mathbf{x}| \sim t^\zeta$. For WD, we have $\zeta = 1/z$, where z is the KPZ dynamic exponent [15], while in the SD limit we have $\zeta = \nu_\perp/\nu_\parallel$ [36], where $\nu_\perp$ and $\nu_\parallel$ are the DP exponents characterizing the scaling of the two correlation lengths of DP clusters [47]: $\xi_\parallel \sim |p - p_c|^{-\nu_\parallel}$ in the longitudinal direction t, and $\xi_\perp \sim |p - p_c|^{-\nu_\perp}$ in the transverse direction x, with $\nu_\perp < \nu_\parallel$. Thus, DP clusters are self-affine and directed paths have a width that scales as $t^{\nu_\perp/\nu_\parallel}$.

That relationship is clearly revealed when we consider the bimodal (0,1) disorder distribution at criticality [34,35]. For $t < \xi_\parallel$, the results of directed polymers and directed percolation are statistically indistinguishable, whereas for $t > \xi_\parallel$ we obtain WD properties [35].

To adapt the arguments used in the (isotropic) OPRL problem to the DPRM problem, we make use of the DP theory.

The optimal directed polymer in the SD limit belongs to the DP cluster that survives (for the first time) at time t in the lattice given by the directed analog of the CPL($w_{\max}$). Equation (8) also applies here but we have to consider the DP analog of the probability density, $\rho_D(p,t)$. In the vicinity of p_c, we have the following results: (i) the survival probability $\Pi_D(p,t) = \int^p \rho_D(p',t)dp'$ decays as $t^{-\delta}$ [48,49], where $\delta = \beta/\nu_\parallel$ and β is the DP critical exponent associated to the order parameter [47]; (ii) the standard deviation of $\rho_D(p,t)$ decreases as $t^{-1/\nu_\parallel}$ [37]; and (iii) $\rho_D(p,t) \sim t^\theta$ with $\theta = 1/\nu_\parallel - \delta$ [37]. In $1+1$ dimensions, we have $\delta \simeq 0.160$ and $\theta \simeq 0.417$ [37,48].

Within the DP cluster, we identify the same types of substructures found in isotropic percolation [50]. We focus on the red bonds, whose properties seem to depend on the constraints and symmetries of the problem. Stenull and Janssen [51] derived the fractal dimension of the set of red bonds in the incipient critical cluster connecting two arbitrary lattice sites. Denoting by $t_\parallel$ the distance between the two sites in the time direction, they obtained $n_{\text{red}} \sim t_\parallel^{d_{\text{red}}}$, with $d_{\text{red}} = (1 + \nu_\perp)/\nu_\parallel - 1$. We can also consider the problem of DP between two opposite sides of a lattice, as in the studies of conductivity in diode networks [52]. It has been claimed [53] that the standard notion of red bonds is ill defined for that problem because of the anisotropy of DP.

In the DPRM geometry, we are interested in the DP cluster that connects the fixed end of the polymer to the transverse x-hyperplane at time t. This DP problem has been studied [49,54,55] and it has been shown that the number of red bonds of the DP cluster surviving after time t, at criticality, has the form

$$n_{\text{red}} \sim t^{1/\nu_\parallel}. \tag{35}$$

This expression is the directed analog of Coniglio's expression [44] for the isotropic case, given in Eq. (10). It is now easy to deduce that the crossover time of the SD-WD transition in the DPRM problem, denoted by $t_\times$, scales as

$$t_\times \sim \left(\frac{\mathcal{P}}{1-\mathcal{P}}\right)^{\nu_\parallel} \quad \text{(DPRM)}. \tag{36}$$

Perlsman and Havlin [25] studied the scaling of this transition for the inverse distribution. They deduced that $\log(W_{\text{opt}}/w_{\max}) \sim t^\theta/a$, and concluded that the SD-WD transition is governed by the ratio $\rho_D(p_c,t)/a$. Their result suggests a crossover time of the form $t_\times \sim a^{1/\theta} = a^{\nu_\parallel/(1-\delta\nu_\parallel)}$ which is different from ours:

$$(t_\times)_{\text{I}} \sim \left(\frac{ap_c}{\ln 2} - 1\right)^{\nu_\parallel} \sim a^{\nu_\parallel}. \tag{37}$$

In $1+1$ dimensions, we have $\nu_\parallel/(1-\delta\nu_\parallel) \simeq 2.396$ and $\nu_\parallel \simeq 1.734$.

We have applied their arguments to the OPRL problem and we have obtained $\log(W_{\text{opt}}/w_{\max}) \sim L^{1/\nu}/a$. Accordingly, the crossover length takes the form $L_\times \sim a^\nu$, which agrees with the result given in Eq. (24). The above result also points to universal function $w_{\max}/W_{\text{opt}} \sim \exp(-z^{1/\nu})$, with $z = L/L_\times$. We have represented this function in Fig. 3(b) by a continuous line. This case corresponds to a Weibull disorder and we observe some deviation with respect to the curve defined by the data collapse. It would be interesting to perform the same analysis for the inverse distribution in the DPRM problem, since a larger deviation might be the cause of the disagreement.

That disagreement seems to be resolved by the results obtained two years later by the same authors [26]. They showed that close to the SD limit, the probability that the optimal directed polymer path is different from the minimal path obtained after applying the max principle is proportional to $t^{2/\nu_\parallel}/a^2$. By making this probability of the order of unity, we deduce $t_\times \sim a^{\nu_\parallel}$, which is in agreement with our result.

C. Undirected polymers

Undirected polymers are fractal in both SD and WD, but the fractal dimension $d_{\rm opt}$ in SD is larger than in WD [19]. This means that they are much more compact in SD conditions. It has been conjectured [19] that the SD limit of UPRM belongs to the same universality class as *maximal* SAWs on the percolation cluster at criticality and critical percolation backbones. Maximal SAWs are the longest SAWs on a percolation cluster.

Our theoretical framework can be readily adapted to the UPRM problem if we take into account the following. In the SD limit, the optimization of our polymer of length ℓ consists of searching the smallest value of w such that the polymer fits in the percolation cluster obtained around the fixed end in the CPL(w). Note that this is satisfied when the maximal SAWs in the cluster have a length larger or equal to ℓ. Thus, the maximal SAW acts as an upper bound for the undirected polymer and this could explain their higher fractal dimension [19]. That smallest value of w obtained in the optimization process is $w_{\rm max}$ and the total weight of the polymer is $W_{\rm opt} = w_{\rm max}$.

Now we apply our arguments to the linear length scale of the UPRM problem, L, which is related to ℓ through the fractal law $\ell \sim L^{d_{\rm opt}}$. Speaking in terms of L, the polymer searches for that CPL(w) which yields a percolation cluster with a correlation length $\xi \sim \ell^{1/d_{\rm opt}}$. Accordingly, the approach to the critical point in the UPRM problem has the form

$$|w_c - w_{\rm max}| \sim L^{-1/\nu} \sim \ell^{-1/(\nu d_{\rm opt})}, \tag{38}$$

which agrees with the theoretical and numerical results presented in Ref. [19].

Once the polymer has found the optimal CPL(w), it selects the minimal weight configuration within the cluster. Whatever it is, the path must pass through all the red bonds in the cluster connecting the starting and ending points, which are separated by a distance that goes as L. From Eq. (22), we deduce that the crossover length $\ell_\times$ of the WD-SD transition in the UPRM problem is

$$\ell_\times \sim \left(\frac{\mathcal{P}}{1-\mathcal{P}}\right)^{\nu d_{\rm opt}} \quad \text{(UPRM)}. \tag{39}$$

In the case of the inverse distribution, we have

$$(\ell_\times)_{\rm I} \sim \left(\frac{a p_c}{\ln 2} - 1\right)^{\nu d_{\rm opt}} \sim a^{\nu d_{\rm opt}}. \tag{40}$$

This law is in perfect agreement with the numerical result obtained by Parshani *et al.* [20] for the inverse distribution.

VII. UNIVERSAL MEASURE OF DISORDER

We finish the paper by returning to the starting point, i.e., to the notion of disorder strength. We have shown that for simple families of distributions it is rather easy to find a parameter S_i that controls the strength of the disorder generated by the family. Typically, it is the so-called *shape parameter*. We now ask if there exists a universal measure S that allows us comparing the disorder strengths of the different families.

This question arises naturally when we consider distributions with several shape parameters, since the contribution of each parameter to disorder is far from being evident. It is the case of the Dagum distribution given in Eq. (7), with two shape parameters β and χ. In Sec. II, we assumed that they contribute in the same fashion and we considered $S_{\rm D} = 1/(\beta\chi)$. This definition, which was enough for previous purposes, is indeed incorrect. In Fig. 8(a), we display the values of $n_{\rm red}^\times$ obtained from the fit of numerical $\mathbf{P}(n, S)$ to the stretched exponential given in Eq. (16). To obtain each set of points, we have fixed one of the exponents to the value indicated in the figure legend and we have let the other one vary. Numerical results are represented against $S_{\rm D}$. In all cases, the asymptotic behavior as we approach the SD limit is linear, as expected, but the prefactor clearly depends on β. The results of the series with fixed χ coincide perfectly with each other, but the results with fixed β show that disorder strength increases as β increases. Thus, our initial assumption is false.

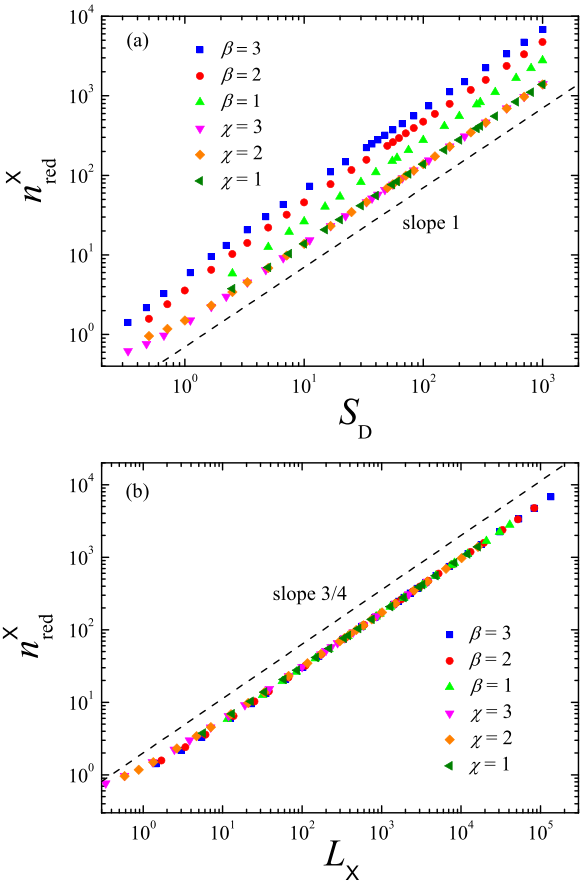

FIG. 8. (a) For the Dagum family, crossover number of red bonds, $n_{\rm red}^\times$, obtained from the fit of $\mathbf{P}(n, S)$ to the stretched exponential function given in Eq. (16), as a function of the disorder parameter $S_{\rm D}$. Each set of results has been obtained by fixing one of the exponents to the value indicated in the legend and varying the other one. The broken line represents linear behavior. (b) Same results but displayed against the crossover length $L_\times$ given in Eq. (41). Broken line represents power-law behavior with exponent $1/\nu = 3/4$. Probability $\mathbf{P}(n, S)$ is obtained from 10^6 realizations of the chain model.

We know that the value of the crossover point $L_\times$, $N_\times$, $t_\times$ or $\ell_\times$, depending on the problem, represents a measure of the extent of the SD limit regime in each problem. Thus, it seems reasonable to think that it could also represent a universal measure of the disorder strength for each case. To check this, we have displayed in Fig. 8(b) the same results shown in Fig. 8(a) but plotted against $L_\times$, which for the Dagum family

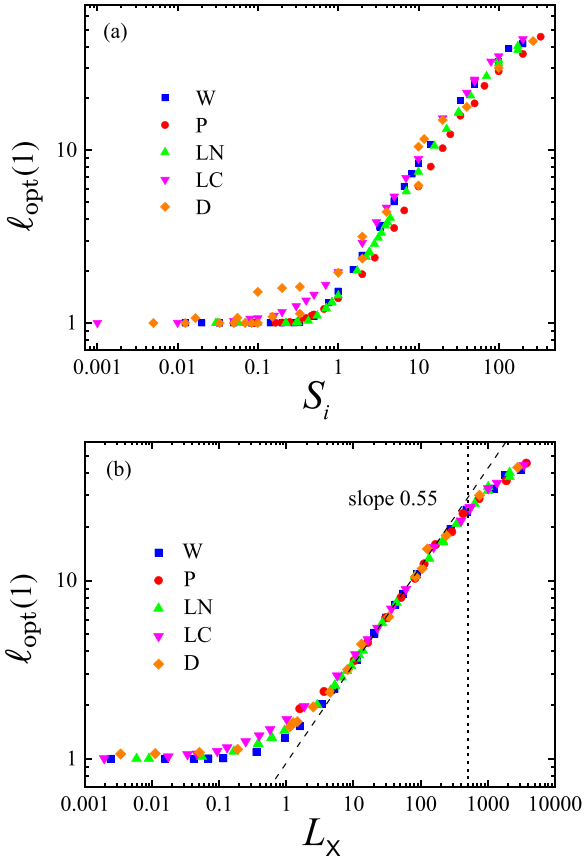

FIG. 9. Average length of the optimal path between the center node and its nearest neighbor in square lattices of linear size $L = 500$ as a function of (a) the corresponding disorder parameter S_i for different families of distributions and (b) the crossover length $L_\times$ given in Eq. (22). Broken line in (b) stands for the scaling law predicted by the unified scaling proposed in Ref. [18]). Vertical dotted line represents the value $L_\times = L$. The averages are over 4×10^4 realizations.

has the form

$$(L_\times)_{\rm D} = \left[\frac{\left(1 - 2^\chi + 2^\chi p_c^{-1/\beta}\right)^{-\beta}}{p_c - \left(1 - 2^\chi + 2^\chi p_c^{-1/\beta}\right)^{-\beta}}\right]^\nu. \qquad (41)$$

The collapse of data is excellent hence supporting our claim.

We show in Fig. 9 another result that supports our conjecture. In square lattices of linear size $L = 500$ centered on the origin, we have measured the average length of the optimal path between the origin and its nearest neighbor, denoted as $\ell_{\rm opt}(1)$, for several families of distributions with different disorder strengths. Disorder parameters S_i were varied from very weak disorder ($S_i \to 0$) to strong disorder ($S_i \gg 1$). In Fig. 9(a), we have plotted the results obtained in our simulations against the disorder parameter of each family. In Fig. 9(b), we have displayed the same results but as a function of $L_\times$ calculated from Eq. (22). In both panels, we appreciate the same qualitative behavior. However, while data dispersion in Fig. 9(a) is quite significant, in Fig. 9(b) the points collapse remarkably well to a universal function, especially in the SD regime $L_\times \gg 1$.

That function can be explained as follows. For $L_\times \ll 1$, we cannot observe SD effects because they happen at scales below the lattice constant. Then, the curve very rapidly approaches the WD limit $\ell_{\rm opt}(1) = 1$ as $L_\times \to 0$. For $L_\times \gg 1$, the effects of disorder are important. We can deduce the expected behavior from the theory presented in Ref. [18]. To do this, we must take into account that both the end-to-end distance and the lattice linear size are fixed, $r = 1$ and $L = 500$, respectively. Hence, the conditions of our problem correspond to the so-called case MD1 (*mixed disorder*). Then we have $\ell_{\rm opt}(1) \sim L_\times^{\kappa/\nu-\varphi}$, with $\kappa/\nu - \varphi \approx 0.55$ in $\mathcal{D} = 2$. The results displayed in the figure are in agreement with that law. The agreement is quite surprising considering that for $r = 1$ one would expect important effects of the lattice discreteness. Finally, when $L_\times$ reaches the system size L, a crossover towards the SD limit behavior takes place (case SD1 in Ref. [18]). In that limit, the optimal path length does not depend on the disorder strength. Our results are again in agreement with the theory. The curve departs from the scaling law when $L_\times$ becomes of the same order as linear size L (indicated in the figure by the vertical dotted line). For $L_\times > L$, the points seem to initiate a slow asymptotic approach towards a constant value (the SD limit).

VIII. CONCLUSIONS AND FURTHER WORK

It is well-known that red bonds may dominate the physics of problems defined on the critical percolation cluster [38,44]. In this paper, we have shown that the SD limit behavior of optimal paths and directed or undirected polymers is another example of it.

This idea is the cornerstone of the unified description for the SD-WD crossover in these problems, which has been proposed here. Since our arguments rely on general properties of the percolation theory, they can be readily adapted to the three problems and, in principle, to any other minimal path problem whose SD limit is related to critical percolation. This is an interesting conjecture that needs validation.

We have obtained that the crossover point is a power-law functional of the disorder function $n_{\rm red}^\times = \mathcal{P}/(1-\mathcal{P})$, with $\mathcal{P} = F(w_c/2)/p_c$. Interestingly, $n_{\rm red}^\times$ conveys information not only on the disorder distribution but also on the topological properties of the network, through term p_c. The scaling exponent of that functional depends on the kind of problem, but in all cases is a function of the connectivity exponent of the corresponding percolation problem, ν for isotropic percolation and $\nu_\parallel$ for directed percolation, which depends only on the dimension. We have shown that our results are in perfect agreement with our simulations and with most of the results reported in the literature, both theoretical and numerical. The very few discrepancies we have found have been analyzed and discussed, although their clarification needs further work.

We have also proposed this crossover point as a universal measure S of the disorder strength in the three problems. We thus have $S_{\rm OPRL} = L_\times$, $S_{\rm OPRN} = N_\times$, $S_{\rm DPRM} = t_\times$, and $S_{\rm UPRM} = \ell_\times$. Our numerical results for the OPRL problem support that conjecture, yet much more work is needed in this regard. Indeed, statistical and topological properties are coupled in that universal measure. This means, for example, that the extent of the SD limit regime in $2\mathcal{D}$ regular lattices with the same disorder distribution depends on the

coordination number. This coupling also appears in related results [31] but has not yet been studied in detail.

That idea was mentioned in Ref. [11]. The authors claimed that link weight structure and topology are orthogonal provided $f(0) \to \infty$. The polynomial distribution with $\alpha < 1$ satisfies that condition and, interestingly, we find that $n_{\mathrm{red}}^{\times}$ depends only on α and not on p_c [see Eq. (32)]. However, there are other distribution families such as the Weibull or the Dagum that also satisfy the condition for certain ranges of their parameters values and yet they lead to a disorder function $n_{\mathrm{red}}^{\times}$ that depend on p_c [see Eqs. (23) and (41)]. This is an interesting question that also deserves further work.

ACKNOWLEDGMENTS

This work was partially supported by Ministerio de Ciencia e Innovación (Spain), Agencia Estatal de Investigación (AEI, Spain, No. 10.13039/501100011033), and European Regional Development Fund (ERDF, A way of making Europe) through Grants No. PID2019-105182GB-I00 and No. PID2021-123969NB-I00. D.V.M. acknowledges Grant No. PRE2019-088226 funded from the same organisms. We acknowledge the computational resources and assistance provided by the Centro de Computación de Alto Rendimiento CCAR-UNED. The authors also thank J. Rodríguez-Laguna and S. N. Santalla for fruitful discussions.

[1] *Statistics of Linear Polymers in Disordered Media*, edited by B. K. Chakrabarti (Elsevier, Amsterdam, 2005).

[2] D. Teodorović and M. Nikolić, Optimal paths, *Quantitative Methods in Transportation* (CRC Press, Boca Raton, 2020).

[3] G. Li, L. A. Braunstein, S. V. Buldyrev, S. Havlin, and H. E. Stanley, Transport and percolation theory in weighted networks, Phys. Rev. E **75**, 045103(R) (2007).

[4] Z. Wu, L. A. Braunstein, S. Havlin, and H. E. Stanley, Transport in weighted networks: Partition into superhighways and roads, Phys. Rev. Lett. **96**, 148702 (2006).

[5] M. Cieplak, A. Maritan, and J. R. Banavar, Invasion percolation and Eden growth: Geometry and universality, Phys. Rev. Lett. **76**, 3754 (1996).

[6] M. Porto, S. Havlin, S. Schwarzer, and A. Bunde, Optimal path in strong disorder and shortest path in invasion percolation with trapping, Phys. Rev. Lett. **79**, 4060 (1997).

[7] V. Rahmani and N. Pelechano, Towards a human-like approach to path finding, Comput. Graph. **102**, 164 (2022).

[8] M. Bockholt and K. A. Zweig, Paths in complex networks, in *Encyclopedia of Social Network Analysis and Mining*, edited by R. Alhajj and J. Rokne (Springer, New York, 2017), pp. 1–11.

[9] P. Van Mieghem, *Data Communications Networking* (Techne Press, Amsterdam, 2006).

[10] H. Wang, J. M. Hernandez, and P. V. Mieghem, Betweenness centrality in a weighted network, Phys. Rev. E **77**, 046105 (2008).

[11] P. Van Mieghem and S. M. Magdalena, Phase transition in the link weight structure of network, Phys. Rev. E **72**, 056138 (2005).

[12] P. Van Mieghem and S. van Langen, Influence of the link weight structure on the shortest path, Phys. Rev. E **71**, 056113 (2005).

[13] B. Fortz and M. Thorup, Optimizing OSPF/IS-IS weights in a changing world, IEEE J. Sel. Areas Commun. **20**, 756 (2002).

[14] R. Mahajan, N. Spring, D. Wetherall, and T. Anderson, Inferring link weights using end-to-end measurements, in *IMW'02: Proceedings of the 2nd ACM SIGCOMM Workshop on Internet Measurement* (Association for Computing Machinery, New York, 2002), pp. 231–236.

[15] T. Halpin-Healy and Y.-C. Zhang, Kinetic roughening phenomena, stochastic growth, directed polymers and all that. Aspects of multidisciplinary statistical mechanics, Phys. Rep. **254**, 215 (1995).

[16] M. A. Henning and J. H. van Vuuren, Optimal paths, in *Graph and Network Theory: An Applied Approach Using Mathematica*, (Springer, Switzerland, 2022), pp. 87–113.

[17] S. Havlin, L. A. Braunstein, S. V. Buldyrev, R. Cohen, T. Kalisky, S. Sreenivasan, and H. E. Stanley, Optimal path in random networks with disorder: A mini review, Physica A **346**, 82 (2005).

[18] D. Villarrubia-Moreno and P. Córdoba-Torres, Unified scaling for the optimal path length in disordered lattices, Phys. Rev. E **109**, 054114 (2024).

[19] L. A. Braunstein, S. V. Buldyrev, S. Havlin, and H. E. Stanley, Universality classes for self-avoiding walks in a strongly disordered system, Phys. Rev. E **65**, 056128 (2002).

[20] R. Parshani, L. A. Braunstein, and S. Havlin, Structural crossover of polymers in disordered media, Phys. Rev. E **79**, 050102(R) (2009).

[21] M. D. Rintoul, J. Moon, and H. Nakanishi, Statistics of self-avoiding walks on randomly diluted lattices, Phys. Rev. E **49**, 2790 (1994).

[22] I. Smailer, J. Machta, and S. Redner, Exact enumeration of self-avoiding walks on lattices with random site energies, Phys. Rev. E **47**, 262 (1993).

[23] N. Schwartz, M. Porto, S. Havlin, and A. Bunde, Optimal path in weak and strong disorder, Physica A **266**, 317 (1999).

[24] A. Hansen and J. Kertész, Phase diagram of optimal paths, Phys. Rev. Lett. **93**, 040601 (2004).

[25] E. Perlsman and S. Havlin, Directed polymer-directed percolation transition: The strong disorder case, Eur. Phys. J. B **43**, 517 (2005).

[26] E. Perlsman and S. Havlin, Stability of directed Min-Max optimal paths, Europhys. Lett. **77**, 20003 (2007).

[27] M. Cieplak, A. Maritan, and J. R. Baravan, Optimal paths and domain walls in the strong disorder limit, Phys. Rev. Lett. **72**, 2320 (1994).

[28] S. V. Buldyrev, S. Havlin, and H. E. Stanley, Optimal paths in strong and weak disorder: A unified approach, Phys. Rev. E **73**, 036128 (2006).

[29] M. Porto, N. Schwartz, S. Havlin, and A. Bunde, Optimal paths in disordered media: Scaling of the crossover from self-similar to self-affine behavior, Phys. Rev. E **60**, R2448(R) (1999).

[30] P. Córdoba-Torres, S. N. Santalla, R. Cuerno, and J. Rodríguez-Laguna, Kardar-Parisi-Zhang universality in first passage

percolation: The role of geodesic degeneracy, J. Stat. Mech. (2018) 063212.
[31] Y. Chen, E. López, S. Havlin, and H. E. Stanley, Universal behavior of optimal paths in weighted networks with general disorder, Phys. Rev. Lett. **96**, 068702 (2006).
[32] S. Sreenivasan, T. Kalisky, L. A. Braunstein, S. V. Buldyrev, S. Havlin, and H. E. Stanley, Effect of disorder strength on optimal paths in complex networks, Phys. Rev. E **70**, 046133 (2004).
[33] S. Sreenivasan, T. Kalisky, L. A. Braunstein, S. V. Buldyrev, S. Havlin, and H. E. Stanley, Transition between strong and weak disorder regimes for the optimal path, Physica A **346**, 174 (2005).
[34] T. Halpin-Healy, Directed polymers versus directed percolation, Phys. Rev. E **58**, R4096 (1998).
[35] E. Perlsman and S. Havlin, The directed-polymer-directed-percolation transition, Europhys. Lett. **46**, 13 (1999).
[36] P. De Los Rios, G. Caldarelli, A. Maritan, and F. Seno, Optimal path and directed percolation, Phys. Rev. E **53**, R2029 (1996).
[37] P. Grassberger and Y.-C. Zhang, "Self-organized" formulation of standard percolation phenomena, Physica A **224**, 169 (1996).
[38] D. Stauffer and A. Aharony, *An Introduction to Percolation Theory*, 2nd ed. (Taylor and Francis, Philadelphia, 2003).
[39] I. Álvarez Domenech, J. Rodríguez-Laguna, R. Cuerno, P. Córdoba-Torres, and S. N. Santalla, Shape effects in the fluctuations of random isochrones on a square lattice, Phys. Rev. E **109**, 034104 (2024).
[40] D. Villarrubia, I. Á. Domenech, S. N. Santalla, J. Rodríguez-Laguna, and P. Córdoba-Torres, First-passage percolation under extreme disorder: From bond-percolation to KPZ universality, Phys. Rev. E **101**, 062124 (2020).
[41] S. V. Buldyrev, S. Havlin, E. López, and H. E. Stanley, Universality of the optimal path in the strong disorder limit, Phys. Rev. E **70**, 035102(R) (2004).
[42] R. M. Ziff, Spanning probability in 2D percolation, Phys. Rev. Lett. **69**, 2670 (1992).
[43] H. E. Stanley, Cluster shapes at the percolation threshold: An effective cluster dimensionality and its connection with critical-point exponents, J. Phys. A **10**, L211 (1977).
[44] A. Coniglio, Thermal phase transition of the dilute *s*-state Potts and *n*-vector models at the percolation threshold, Phys. Rev. Lett. **46**, 250 (1981).
[45] L. A. Braunstein, S. V. Buldyrev, R. Cohen, S. Havlin, and H. E. Stanley, Optimal paths in disordered complex networks, Phys. Rev. Lett. **91**, 168701 (2003).
[46] R. Cohen, D. ben-Avraham, and S. Havlin, Percolation critical exponents in scale-free networks, Phys. Rev. E **66**, 036113 (2002).
[47] *Fractals and Disordered Systems*, edited by A. Bunde and S. Havlin, 2nd ed. (Springer, Berlin, 1996).
[48] I. Jensen, Low-density series expansions for directed percolation: I. A new efficient algorithm with applications to the square lattice, J. Phys. A **32**, 5233 (1999).
[49] K. B. Lauritsen, K. Sneppen, M. Markošová, and M. H. Jensen, Directed percolation with an absorbing boundary, Physica A **247**, 1 (1997).
[50] W. Kinzel, Directed percolation in *Percolation Structures and Processes*, edited by G. Deutscher, R. Zallen, and J. Adler, Ann. Isr. Phys. 5 (Hilger, Bristol, 1983).
[51] O. Stenull and H.-K. Janssen, Nonlinear random resistor diode networks and fractal dimensions of directed percolation clusters, Phys. Rev. E **64**, 016135 (2001).
[52] S. Redner, *Percolation and conduction in random resistor-diode networks, in Percolation Structures and Processes*, edited by G. Deutscher, R. Zallen, and J. Adler, Ann. Isr. Phys. 5 (Hilger, Bristol, 1983).
[53] J. Schmittbuhl, G. Olivier, and S. Roux, Multifractality of the current distribution in directed percolation, J. Phys. A **25**, 2119 (1992).
[54] G. Huber, M. H. Jensen, and K. Sneppen, Distributions of self-interactions and voids in (1+1)-dimensional directed percolation, Phys. Rev. E **52**, R2133 (1995).
[55] A. C. Barato and H. Hinrichsen, Directed percolation with a single defect site, J. Stat. Mech. (2011) P02035.